Efficient removal of fluoride ions present in industrial effluents using metal-organic frameworks of UiO-66-NH2

Dario Lacalamita, Guillaume Hoyez, Chiara Mongioví, Anne Ponchel, Nadia Morin-Crini, Cyril Rousseau, Christophe Loup, Jolanta Rousseau, Marina Raschetti, Eric Monflier, et al.

▶ **To cite this version:**

Dario Lacalamita, Guillaume Hoyez, Chiara Mongioví, Anne Ponchel, Nadia Morin-Crini, et al.. Efficient removal of fluoride ions present in industrial effluents using metal-organic frameworks of UiO-66-NH2. Journal of Water Process Engineering, 2023, 53, pp.103791. 10.1016/j.jwpe.2023.103791 . hal-04102244

HAL Id: hal-04102244
https://univ-artois.hal.science/hal-04102244

Submitted on 15 Nov 2023

HAL is a multi-disciplinary open access archive for the deposit and dissemination of scientific research documents, whether they are published or not. The documents may come from teaching and research institutions in France or abroad, or from public or private research centers.

L'archive ouverte pluridisciplinaire **HAL**, est destinée au dépôt et à la diffusion de documents scientifiques de niveau recherche, publiés ou non, émanant des établissements d'enseignement et de recherche français ou étrangers, des laboratoires publics ou privés.

Efficient removal of fluoride ions present in industrial effluents using metal-organic frameworks of UiO-66-NH_2

Dario Lacalamita[a], Guillaume Hoyez[b], Chiara Mongioví[a], Anne Ponchel[b], Nadia Morin-Crini[a], Cyril Rousseau[b], Christophe Loup[a], Jolanta Rousseau[b], Marina Raschetti[c], Eric Monflier[b], Vincent Placet[c], Grégorio Crini[a,*]

[a]Laboratoire Chrono-environnement, UMR 6249, Université de Franche-Comté, 16 route de Gray, 25000 Besançon, France; ORCID: 0000-0002-4819-1104

[b]Univ. Artois, CNRS, Centrale Lille, Univ. Lille, UMR 8181, Unité de Catalyse et Chimie du Solide (UCCS), 62300 Lens, France

[c]FEMTO-ST, Department of Applied Mechanics, Université de Franche-Comté, 25000 Besançon, France

Corresponding Author

Email address: gregorio.crini@univ-fcomte.fr (G. Crini) ORCID: 0000-0003-2540-6851

ABSTRACT

In this last decade, numerous works have been published on the use of metal organic frameworks (MOFs) for applications in adsorption field to remove contaminants from aqueous solutions. However, little is known about MOFs as adsorbents for the removal of fluoride ions from real effluents. In this work, a highly porous MOF, UiO-66-NH_2, was used for the final treatment of complex discharge waters containing fluoride ions from a surface treatment plant. Batch experiments showed that MOF exhibited high adsorption capacities towards fluoride ions, leading to concentrations under current regulation values. 70-80% of the fluoride was removed in 60 min using 100 mg of MOF in 50 mL of effluent without changing the industrial initial pH. At the same time, the treatment also completely eliminated traces of aluminium in the discharge water. All the results showed that adsorption onto a non-conventional material

such as UiO-66-NH_2 can be an interesting tertiary treatment step to remove more pollutant streams from multi-contaminated industrial discharge waters.

Keywords:

UiO-66-NH_2

Fluorides

Aluminium

Adsorption

Industrial effluents

1 Introduction

Among the nanomaterials studied in the literature, the field of metal-organic frameworks (MOFs) has become one of the fastest growing areas of chemistry due to their remarkable physical, structural, and chemical properties, and above all their high potential for applications in a wide range of industrial fields, for example in gas separation/storage, drug delivery, sensing (luminescent sensors), catalysis, and photocatalysis. This is reflected by the ever-increasing number of new structures offered and articles published on the subject [1-11]. MOFs are tunable crystalline organic-inorganic hybrid networks with adsorption capacity properties superior to those of conventional commercial materials such as activated carbons, silicas, activated aluminas, and zeolites. They also possess numerous intrinsic characteristics such as high porosity with a well-controlled pore size distribution, high surface area, and low density. In addition, their non-toxicity, structural malleability, flexibility, versatility and adaptability to many different conditions and applications make them particularly attractive [12-14]. This new class of porous materials with unprecedented functional characteristics can be used in various fields related to adsorption including gas removal, CO_2 adsorption, hydrogen storage, and water and wastewater treatment [15-23].

A review of the literature data on the use of MOFs as adsorbents in batch processes for water treatment applications shows that MOFs are indeed effective in complexing contaminants, particularly metals, metalloids, and radionuclides [24-34]. MOFs have also been evaluated for their ability to remove dyes, pharmaceuticals and personal care products, pesticides and

agrochemicals, phenols, phosphates, and fluoride ions from water [19,35-45]. In general, MOFs show high removal or recovery performance towards a wide variety of inorganic and organic substances. However, the survey of the literature data also shows that the efficiency depends on the characteristics of the materials, the experimental conditions of the batch (often not very detailed) and the solutions to be treated, notably the pH and the dose of the adsorbent. Some results from identical materials studied under similar experimental conditions are also contradictory. In addition, the vast majority of published results have been obtained using standard solutions, often monocontaminated, prepared in the laboratory under controlled conditions [35,43,46,47]. Indeed, to our knowledge, there are few studies obtained from industrial waters [35,47,48].

In Europe, the surface treatment industry is still considered as one of the main consumers of water and energy resources, and therefore a major polluter. These industries produce huge quantities of highly loaded wastewater containing inorganic and organic pollutants, including anions (fluoride and cyanide ions) from cleaning, polishing and passivation operations, cations (metals and metalloids) from plating and anodising baths, and organic matter from oils, greases, and solvents. Before being discharged into the environment, this industrial wastewater must comply with specific regulations. It is therefore treated in wastewater treatment plants, usually by chemical precipitation techniques coupled with adsorption and filtration stages. However, even if they comply with the regulations in force, these treated waters still contain a mixture of chemical substances. Moreover, these contaminant discharges are not consistent either in quality or quantity and can have adverse effects on aquatic ecosystems. One of the substances particularly monitored by the powder coating industry, a particularly important activity in France, is fluorides, with an emission limit value set at 30 mg/L. However, the regulations are constantly changing, hence the need to find methods capable of eliminating these fluorides, in order to anticipate any change in this emission limit value.

Complementary water treatment techniques to remove fluorides and to move towards zero discharge are known: adsorption on aluminas, chelation on resins, membrane filtration, etc. How to choose? As recently discussed by Crini and Lichtfouse [49], the answer is difficult for small companies for technical and economic reasons. Moreover, from a water engineering perspective, the challenge is also difficult because the pollutants to be treated, such as fluorides, are found in trace amounts in complex mixtures containing other elements such as metals. In addition, the substances interact with each other to form complexes, which does not favour their elimination. Finally, the waters to be treated have basic pH values (close to 8) and are highly

saline with large quantities of salts (close to marine salinity). It is therefore difficult to find adsorbent materials capable of selectively eliminating the fluorides present in such conditions. Innovation is therefore needed to propose materials capable of meeting these challenges. Nanomaterials, such as MOFs, which are already used in many areas of our daily lives (electronics, cosmetics, health sector), could be a solution to environmental pollution problems such as fluorides.

MOFs correspond to a versatile and efficient family of adsorbents, generally associated with high porosity, surface area and stability in water. MOFs are generally built from metal-oxo clusters bridged together by multidentate organic linkers (typically dicarboxylate ligands). In this context, we have selected the UiO-66-NH_2 MOF, which is a zirconium-based metal-organic framework consisting of $[Zr_6O_4(OH)_4]^{12+}$ building units linked together by 2-aminoterephthalate carboxylates. These zirconium-based MOFs are some of the most widely used stable materials that have been tested for several applications, including the decontamination of water, mainly because of their stability, variety of structures, and relatively easy synthesis and modification while preserving the morphology of the MOF. In addition, this MOF family has a high degree of coordination of metal cluster, especially the Zr-UiO-66-NH_2 MOFs, which are known for their exceptional water stability over a large range of pH. Their production in large quantities is well mastered in green conditions, i.e., in aqueous medium without harmful organic solvents, and at conventional temperature and pressure. Zr-MOFs also presents a low toxicity and are environmentally compatible. The UiO-66-NH_2 is also expected to facilitate the adsorption of fluorides via electrostatic attractions and hydrogen bonding due to the presence of amino groups [12-15,21-24,35-41].

In this work, we studied the decontamination performance of a UiO-66-NH_2 MOF material to remove fluoride ions present in polycontaminated water from an industrial powder coating process with the objective of selectively decreasing the fluoride ions complexed with metals such as aluminium and significantly lowering the discharged flux. The removal capabilities of the material were first studied on standard solutions under controlled conditions containing known concentrations of fluorides in presence or absence of aluminium. The tests were then carried out on industrial discharge waters (DWs) from the outlet of a physicochemical wastewater treatment plant. Finally, the effect of several parameters (initial fluoride concentration in DWs, adsorbent dosage, and contact time) on the performance was studied in order to optimize the conditions of the proposed treatment.

2 Experimental

2.1 Chemicals

All solvents, salts and reagents were commercially purchased and used as received without further purification. Zirconium (IV) oxychloride octahydrate ($ZrOCl_2 \cdot 8H_2O$, 99.5 %), *N,N*-dimethylformamide (DMF, 99.8 %) were purchased from Sigma-Aldrich (Quentin-Fallavier, France). 2-aminoterephthalic acid ($H_2BDC\text{-}NH_2$, purity > 99 %) was purchased from Acros Organics - Fisher Scientific (Illkirch, France) or Strem Chemicals (Bischheim, France). Acetic acid was provided by Fisher Scientific (France) while absolute methanol and ethanol were purchased from Verbiese (Merville, France).

2.2 Modulated hydrothermal synthesis of UiO-66-NH_2

The hydrothermal synthesis of UiO-66-NH_2 was performed according to a protocol previously reported by some of us [50]: $ZrOCl_2 \cdot 8H_2O$ (10.30 g, 10 mmol) was first dissolved in a mixture of water/acetic acid (150 mL/150 mL) at 90 °C. 2-aminoterephthalic acid (10 mmol) was added to the previous mixture and the reaction was further heated at 90 °C for 24 h. The precipitate was washed successively with DMF (2 × 50 mL), water (2 × 50 mL) and methanol (2 × 50 mL) and finely let overnight in methanol (150 mL) in order to remove residual reagents from the MOF pores. In a final step, the sample was dried under vacuum at 100 °C for 24 h to yield the final UiO-66-NH_2 product.

2.3 UiO-66-NH_2 structure stability control (static conditions)

The stability test was performed by using 100 mg of UiO-66-NH_2 suspended in 200 mL of industrial effluent and the mixture was left to stand different times (2 h, 1 day, 1 week) at room temperature without stirring. MOF was isolated by centrifugation and dried at 100 °C overnight.

2.4 Characterization methods

X-Ray Diffraction (XRD) measurements were performed using a Rigaku ULTIMA IV diffractometer equipped with a Cu anticathode (Kα = 1.5418 Å), Soller slits to limit the divergence of X-ray beam and a nickel foil filter to attenuate the Cu Kβ line. XRD patterns were recorded in the 2θ range of 3-50° (scan speed of 0.4° min^{-1}) using the Bragg-Brentano configuration. Fourier transform infrared (FT-IR) experiments were performed using a Spectrum Two Perkin-Elmer FT-IR spectrometer equipped with a single-reflection diamond module (ATR) and a deuterated triglycine sulfate detector. FTIR spectra were recorded in the wavenumber range of 400-4000 cm^{-1}. N_2 adsorption-desorption isotherms were collected at 196°C using an adsorption analyzer Micromeritics Tristar II 3020. Prior to analysis, 80-100 mg of a freshly dried sample (100°C, overnight) was degassed for 2 h at 100°C under vacuum. For

the surface area determinations, the Langmuir and Brunauer-Emmett-Teller (BET) models were applied to fit the experimental data. The BET specific surface areas were determined in the P/P^0 range from 0.001 to 0.05, identified by applying the four consistency criteria developed by Rouquerol et al. [51] (i) the BET C constant should be positive; (ii) the function V(1- (P/P°)) should continuously increase with P/P°; (iii) the monolayer capacity (V_m) should correspond to a relative pressure P/P° included within the selected pressure; (iv) the calculated value for monolayer formation ($1/(\sqrt{C} + 1)$) should be approximately equal to P/P° at the monolayer formation (a tolerance of 20% has been accepted). In all cases, the four consistency criteria were satisfactorily fulfilled. The t-plot method was used to estimate the amount of micropores based on the Halsey thickness equation. The total pore volumes were estimated from the adsorbed amounts at a relative pressure of ca. 0.95. Based on the N_2 adsorption data, a nonlocal density functional theory (NLDFT) model included in the commercial Tristar II 3020 V1.03 software was used for the calculation of pore size distributions (assuming slit pore geometry). The surface zeta potential of UiO-66-NH_2 was measured by Malvern Nano ZS Zetasizer at a controlled temperature (25 ± 0.1 °C). The measurements are based on a Laser Doppler electrophoretic mobility of the MOF via the Helmholtz-Smoluchowski equation $\xi = (\eta/\varepsilon)\cdot\mu_e$, where μ_e corresponds to the ratio between the velocity of the heterogeneous sample and the magnitude under the used electric field, η represents the viscosity and ε is equal to the dielectric constant of H_2O. For this study, 2 mg MOF were dispersed into 10 mL of deionized water to have a mass concentration of 0.2 g/L of MOF in every flask. pH of each mixture (1.98, 3.03, 4.05, 4.96, 6.02, 6.99, 8.06, and 9.01) was adjusted by adding some drops of sodium hydroxide or hydrochloric acid solution (10^{-2} mol/L both). Before analysis, each mixture was kept during 5 min under ultrasound. Control of pH was performed after 30 min of equilibrium (without change of pH). 2 mL of these different mixtures were put in a zeta potential cell. 3 measures were collected for each unity of pH (an average was done to have the value of zeta potential (ζ) for each unity of pH) after 5 min of equilibrium in the cell. The plotting of $\zeta = f(pH)$ leads to the determination of the pH of point of zero charge (pH_{PZC}). The surface images were acquired with a scanning electron microscope ApreoS (ThermoFisher Scientific, France) in a low vacuum mode (0.5 mbar H_2O) to avoid charging effects. The elemental analyses were performed by energy dispersive spectroscopy with an UltraDry EDS (ThermoFisher Scientific, France) at 20 kV. Surface observations and analysis were both carried out by adding a specific X-ray cone on the final lens, in order to minimize the electron path and reduce the beam scattering within the chamber in low-vacuum mode.

2.5 Industrial effluents

The experiments were carried out on water discharged by a local industry that deals with the final treatment of large aluminium plates, mainly for architectural purposes, by cleaning, passivating and painting these surfaces. For this, the company uses large volumes of water (~70-80 m^3/day) and chemicals such as fluoride baths, generating similar volumes of raw wastewater contaminated by fluorides (the main problem) and metals, which must be purified before discharge. The fluoride baths, consisting of ammonium salts complexed in a strong acid or fluorides doped with boron, are essential in industrial processes to attack aluminium and keep it in solution. These reactions guarantee the anti-corrosion properties of the profiles.

To achieve the desired pollutant removal in the most economical way, the general treatment scheme for industrial process wastewater involves the following five main steps [52,53]:

(i) a chemical pre-treatment to decomplex the pollutants (this step is important to "liberate" fluorides as they are known to form stable complexes with other chemical entities present in process water, which makes their precipitation difficult);

(ii) another pre-treatment using calcium carbonate followed by precipitation using lime to convert soluble fluoride and metal (mainly aluminium) ions into their insoluble form;

(iii) if, following these chemical treatments, the residual concentrations of metals (aluminium) and especially organic load (COD) are high, a fixing agent in powder form (activated carbon, mineral filler or a co-precipitating agent) is then added to the precipitation tank to improve the purification efficiency of the process;

(iv) the treated waters are then collected and flocculated using an anionic polymer and they are finally decanted before being discharged into the aquatic environment if they comply with the regulations in force;

(v) finally, the resulting sludge is sent to a specific site for proper disposal.

In this work, 9 samples (denoted DW1-DW9) were collected at the wastewater treatment plant disposal outlet over a period of 3 months (3 effluents on 3 consecutive days were collected each month), each effluent being an average sample characteristic of that day's activity. Their analytical characteristics are described in Table 1 and these values represent the minimal and maximal concentrations (expressed in mg/L, with the exception of nonylphenols in µg/L) determined for the 9 effluents studied. The main concern for the industrial is the concentrations of fluorides, discharge standards being fixed at 30 mg/L. The industrial must also respect the emission limit values for other pollutants, in particular metals, as described in Table 1.

Table 1

Minima and maxima (mean ± standard deviation) for several parameters and pollutants over 9 industrial discharge waters (DWs) taken during the sampling campaign and the corresponding legal discharge limits (samples characteristic of that day's activity).

Pollutant / Parameter	Unit	LQ[d]	Nine DWs	Limit emission value[a]
Water flow	m^3/day		29-80 (63 ± 17)	<100
pH at 20°C			7.7-8.1 (7.9 ± 0.2)	6.5-9
Suspended solids	mg/L	2	6.2-24 (10.4 ± 5.4)	<25
Chemical Oxygen Demand	mg/L	2	35-181 (87 ± 43)	<150
Easily released cyanides[b]	mg/L	0.01	<LQ[d]	<0.1
Fluorides	mg/L	0.17	6.9-25 (14.8 ± 6)	<30[c]
Al	mg/L	0.014	0.39-1.2 (0.67 ± 0.28)	<5
Zn	mg/L	0.0002	<LQ[d]	<3
Cu	mg/L	0.003	<LQ[d]	<2
Ni	mg/L	0.001	0.005-0.01 (0.0061 ± 0.0022)	<2
As	mg/L	0.004	<LQ[d]	<1
Fe	mg/L	0.001	<LQ[d]	<5
Cr III	mg/L	0.0002	<LQ[d]	<0.9
Cr VI	mg/L	0.01	<0.01	<0.1
Ti	mg/L	0.0008	0.005-0.01 (0.008 ± 0.007)	<2
Nonylphenols	µg/L	0.01	<LQ[d]	-

[a] Mean daily output for direct outflow (French law of 5th September 2006).
[b] Free or complexed cyanides dissolved in water.
[c] For a flow of <100 m^3/d.
[d] Limit of quantification.

2.6 Batch experiments

The experiments were conducted on industrial wastewaters using the batch method without changing the effluent initial pH (7.9 ± 0.2) in order to simulate the industrial process. 100 mg of MOF were added in 50 mL of discharge waters in a tightly closed flask, and the solution was stirred on a thermostatic mechanical shaker operating at a constant agitation speed (250 rpm), for 1 h at room temperature (22 ± 1°C). This time of 60 mins was chosen because it corresponds to the contact time used by the industry in its treatment plant. After treatment, the MOF was then removed by filtration and the concentration of the solution was determined. The adsorption performance, representing the ratio between the amount of adsorbed pollutant and the starting amount of pollutant, is finally calculated and expressed in percentage abatement/removal (% R) or in amount of pollutant adsorbed at time t by 1 g of MOF (q_t in mg/g). MOF dosage was

varied between 0.025 and 0.1 g to investigate its effect on the biosorption capacity. Studies were also conducted for various time intervals (ranging from 1 to 120 min) to determine when adsorption equilibrium was reached. Preliminary studies were carried out on standard solutions containing fluoride and aluminium at concentrations of 25 and 5 mg/L respectively, under the same batch conditions (100 mg MOF in 50 mL, 60 min stirring). Mono-contaminated and binary solutions containing these two elements were thus studied and compared to real waters. It was noted that, at the end of the adsorption process, a significant pH variation of 1 unit was observed in each experiment for the real waters while this variation reached 3 units for the synthetic solutions.

2.7 Analytical methods

The pH of each sample was measured using a portable pH meter (3110 model, WTW, Alès, France). Al was measured using rapid test kits by a portable photometer (Spectroflex 6100 model, WTW, Alès, France) and results were directly expressed in mg/L. Al concentration was also determined by inductively coupled plasma atomic emission spectroscopy (ICP-AES, ThermoFisher, iCAP 6500, Courtaboeuf, France). Fluoride concentrations were measured by rapid test kits using a portable photometer (Spectroflex 6100 model, WTW, Alès, France), by ion chromatography (ThermoFisher, France) and by selective detection using a fluoride ion-selective electrode (Hach, IntelliCAL ISEF121, France). In all cases, the Al and F measurements gave comparable values.

2.8 Reproducibility of adsorption data

For real waters, all experiments were run in triplicate and found reproducible (experimental error within 3%). In each figure showing the adsorption data is shown the standard deviation of the mean obtained on the three replicates. Blanks were also run without any material to determine the extent of pollutant removal by containers (no adsorption was observed).

3 Results and discussion

3.1 Characterization of the MOF materials

The XRD and BET analysis were performed to elucidate the structural and textural properties of UiO-66-NH_2 (Fig. 1) and were in agreement with the literature data [54,55]. According to the XRD pattern, the most intense characteristic diffraction peaks of UiO-66-NH_2 at 2θ = 7.34°, 8.52° and 25.76° indexed with (111), (002) and (006) crystal planes, respectively, confirm the face-centred-cubic topology with the Fm-3m space group as the unique crystalline phase [50]. Furthermore, the presence of sharp characteristic peaks indicates a high degree of crystallinity in

obtained MOF. The BET analysis by N_2 adsorption-desorption isotherm reveals a typical type I isotherm with H4 hysteresis loop proving the microporous structure of solid, with a size of the pores below 20 Å. The enhance crystallinity was confirmed by high BET surface area about 945 g/m^2. The SEM images (Fig. 2), used for the characterization of the morphology of the UiO-66-NH_2 crystals, showed an agglomeration of the uniformed shaped particles with a size in the range of 1.5-2 µm.

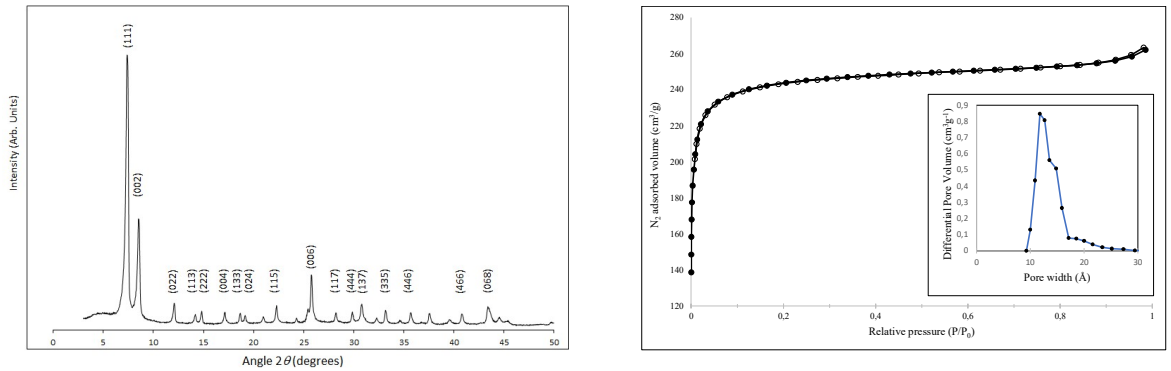

Fig. 1. XRD pattern (left) and N_2 adsorption-desorption isotherms collected at 77 K (right) of UiO-66-NH_2.

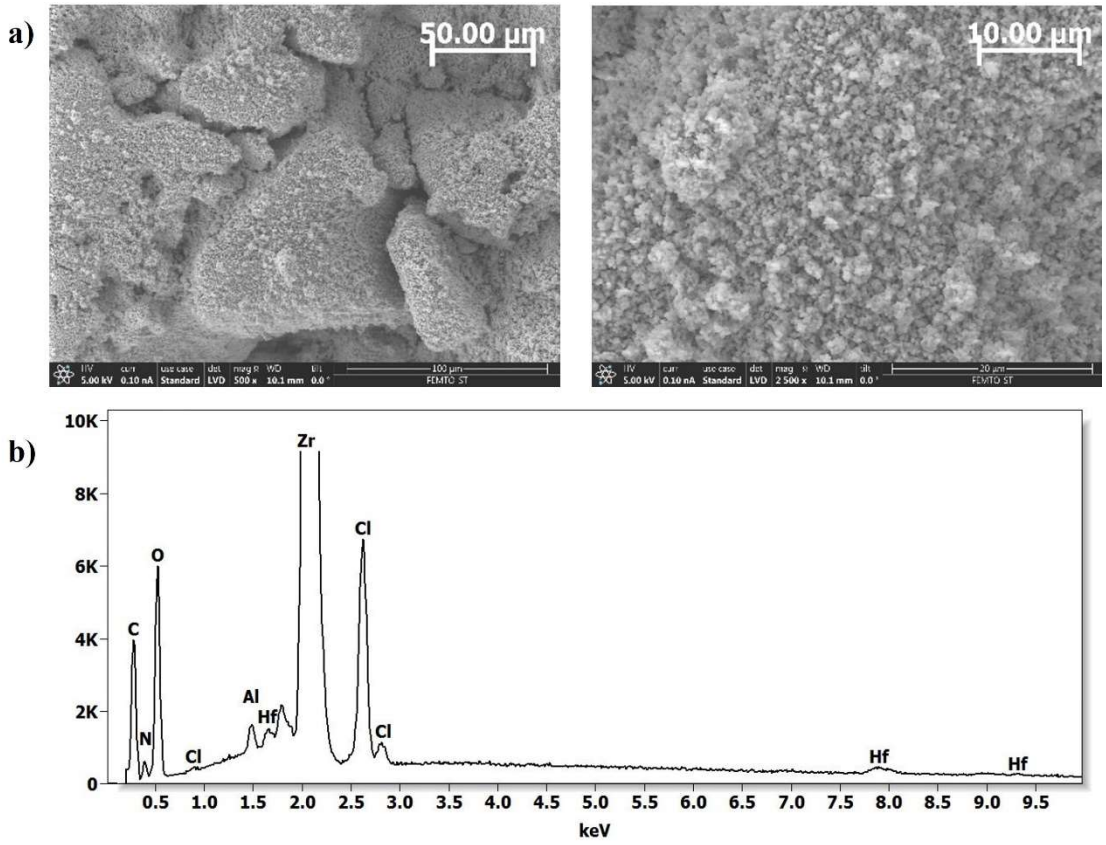

Fig. 2. (a) SEM images at two different magnifications (x500 and x2500) and (b) corresponding EDX data of UiO-66-NH_2.

The evolution of zeta potential (ζ) was measured on the UiO-66-NH_2 sample dispersed in aqueous solution considering pH ranging from 2 to 9. The results in Fig. 3 indicated a value of 7 for the pH of the point of zero charge (pH_{PZC}). Below this value, the surface is positively charged leading to the adsorption of the anions by electrostatic attractions. While for a pH > 7 value, the surface is rather negatively charged promotes the adsorption of cations. At the pH_{PZC} point, the surface has a surface charge density of zero favoring the aggregation of particles. This behavior agrees the protonation steps of zirconium cluster. A similar isoelectric point has been published [37].

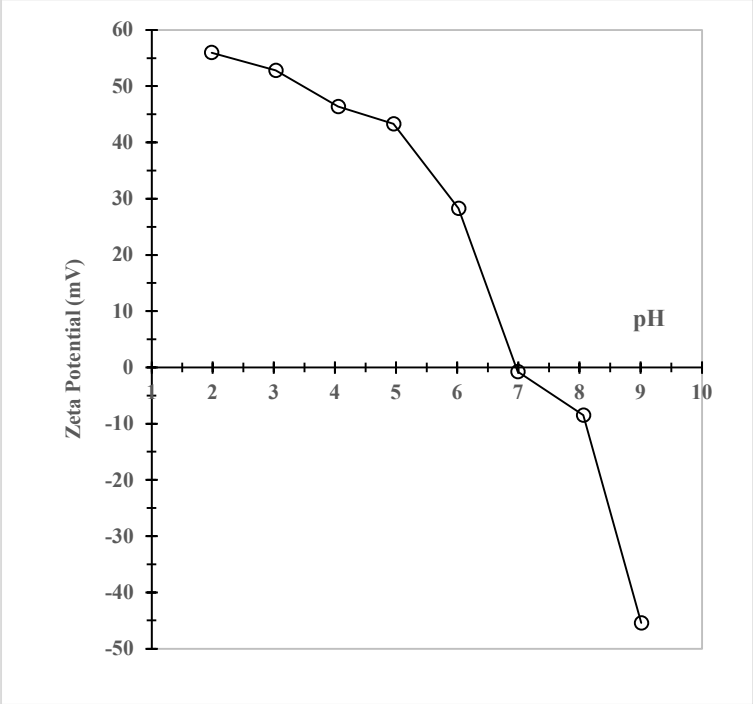

Fig. 3. Zeta potential of UiO-66-NH_2 evolution in aqueous solution at different pH values.

3.2 Chemical composition of discharge waters

The first aim of this study was to identify and quantify the levels of fluorides and metals present in the 9 samples. Table 1 reports the levels of the inorganic species present in the 9 considered wastewaters (DW1-DW9), such as fluorides and metals, during our sampling campaign. It is clear that the physicochemical treatment process used by the industrial for its wastewaters treatment ensures an efficient purification, lowering the pollutant load at

satisfactory levels for the current regulation limits. The F content is reduced to a level well below the legal limit (30 mg/L), with an average of 14.8 ± 6 mg/L. However, of the 9 effluents studied, some such as DW1, DW8 and DW9 have notable fluoride concentrations (Table 1). This indicates that the physicochemical treatment is highly variable for their removal in terms of performance, resulting in varying fluoride concentrations. It is known that, by conventional chemical precipitation, the fluoride concentration in an industrial effluent cannot be reduced, working under optimal conditions, to ≤ 20 mg/L without the help of dilution with fresh water. Indeed, it is precipitated as CaF_2 by the addition of $Ca(OH)_2$, assisted by $CaCl_2$, but the solubility product of the salt is relatively low (Ks = 3.5 10^{-11}) allowing the presence in the solution of at least 8 mg/L of fluorides [52,53]. In addition, the physicochemical treatment is very efficient for the removal of metals such as Al, Zn, Cu, Ni, As, Fe and Cr. These species have concentrations well below the regulations (Table 1). For example, the Al content with an average of 0.67 ± 0.28 mg/L has been greatly reduced, below its limit value (5 mg/L). These results show that the physicochemical treatment results in discharges that certainly comply with the regulations but still contain variable polycontamination, requiring the installation of additional treatment to further reduce pollution. Moreover, the industrialist must propose actions to reduce fluoride discharges in the coming years, as the limit value for fluoride emissions will be reduced from 30 to 20 mg/L. In this context, the 9 samples considered were subjected to adsorption using MOF materials designed for this purpose.

3.3 Synthetic solutions

Preliminary studies were carried out on standard solutions containing fluoride and aluminium at concentrations of 25 and 5 mg/L respectively under the same batch conditions. For fluoride species present in synthetic solutions, the results showed that 100 mg MOF were able to remove all the element present in the solution (% removal > 95%) and they were found reproducible (n = 6). This result demonstrates the presence of strong interactions between protonated amine functions and fluorides [22,24,35,40,45]. Lin et al. [35], in studying fluoride adsorption onto UiO-66-NH_2 (batch conditions: 10 mg of MOF in 20 mL of F synthetic solution at 20 mg/L), also reported the presence of this type of interaction. Zhang et al. [43] studied the adsorption of phosphates on a similar MOF (batch conditions: 20 mg of MOF in 10 mL of PO_4^{3-} synthetic solution at 20 mg/L with pH = 2-12) and explained their results by both the presence of complexation due to interactions between amine functions and phosphates and hydrogen bonds. Ahmadijokani et al. [40], in their comprehensive review on the application of MOFs in water treatment, also reported mainly an adsorption mechanism via electrostatic interactions.

For a binary mixture containing fluoride and aluminium, the presence of aluminium did not affect the removal of fluoride (% removal > 90%, n = 3). Indeed, even in the presence of aluminium at a concentration of 5 mg/L, the MOF is able to adsorb the 25 mg/L of fluoride. However, no adsorption results were obtained for aluminium present in monocontamined solution. This can be explained by the acidic pH of the solution (Table 2). When MOF is added to the synthetic solution, a significant decrease in pH was observed, as well as at the end of the adsorption. At this pH, the aluminium remains in a stable cationic form and therefore does not interact with the MOF. This interpretation is in agreement with the pH of zero point charge of the material. It was found that for the real waters, the change in pH after the addition of the MOF material and at the end of the adsorption process was relatively smaller (Table 2). Nevertheless, a decrease of 1 pH unit was systematically observed for all 9 discharges.

Table 2

Variation of pH values of synthetic solutions and discharge waters before and after adsorption (mean and standard deviation for n samples).

	Initial pH	**n**	**After adsorption at t = 0 min**	**After adsorption at t = 60 min**
Synthetic solutions	6.1 ± 0.2	6	3.6 ± 0.2	3.1 ± 0.3
Discharge waters	7.3 ± 0.4	9	6.4 ± 0.2	6.2 ± 0.4

3.4 Treatment of discharge waters by adsorption on a MOF material

Results are reported in Fig. 4 in terms of pollutant concentration before and after adsorption treatment on MOF for each studied sample. For both fluorides and aluminium, the results before adsorption show the significant chemical variability of the discharges, with F concentrations ranging from 6.9 to 25 mg/L and Al concentrations from 0.39 to 1.2 mg/L. For the 9 discharge waters studied, the F and Al average concentrations are respectively 14.8 ± 6 and 0.67 ± 0.28 mg/L. After adsorption on the MOF material, these average decrease to 3.7 ± 1.8 for F and 0.01 ± 0.007 for Al, which corresponds to an abatement of 75% for F and 98% for Al. These results demonstrate the effectiveness of MOF in removing fluorides from polycontaminated mixtures. Furthermore, whatever the discharge water, the fluoride concentration values obtained are well below the emission limit value of 30 mg/L. It is interesting to note that MOF is able to remove trace amounts of aluminium from real water, whereas in synthetic solution no % removal was obtained. This result is consistent with the fact that chemicals present in discharges interact with each other to form complexes. It is known that fluorides can form complexes with other cations and substances present in industrial waters [52,53].

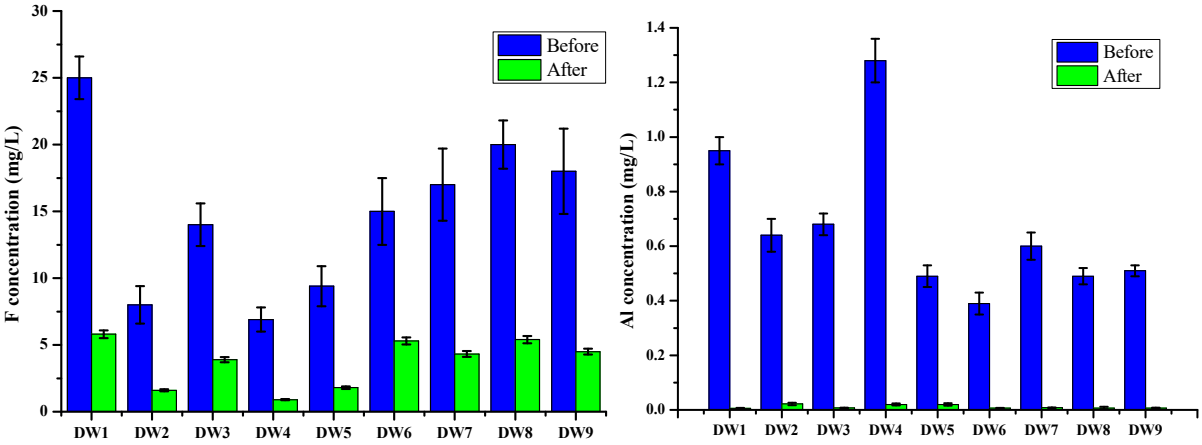

Fig. 4. Comparison for fluoride (left) and aluminium (right) concentrations in discharge waters before and after adsorption onto UiO-66-NH_2 (conditions: 100 mg of MOF in 50 mL of industrial water; contact time = 60 min; n = 3).

The results in Fig. 5 compare the removal (expressed in % abatement) of fluorides and aluminium present in a discharge water by changing the dose of MOF in 50 mL of water without changing the industrial initial pH and keeping the other parameters of the batch constant. The initial F and Al concentrations for this real water were 20 and 0.5 mg/L. As expected, by increasing the amount of adsorbent from 25 mg to 100 mg, the removal percentage of fluorides increased significantly from 34 % at a dose of 25 mg to 70 % at 100 mg. This result can be explained by the increase in complexation sites that favour interactions between protonated amine functions and fluorides [35,40]. For Al, an increase in the dose had no effect. A dose of 75 mg in 50 mL is sufficient to obtain a result. At this dose, the final concentrations of F and Al after adsorption were 7 and 0.1 mg/L respectively, values well below the regulatory concentrations. This experiment was repeated with another discharge water containing 17 mg fluoride and 0.3 mg aluminium per liter and similar results to those shown in Fig. 5 were found, showing the reproducibility of the data.

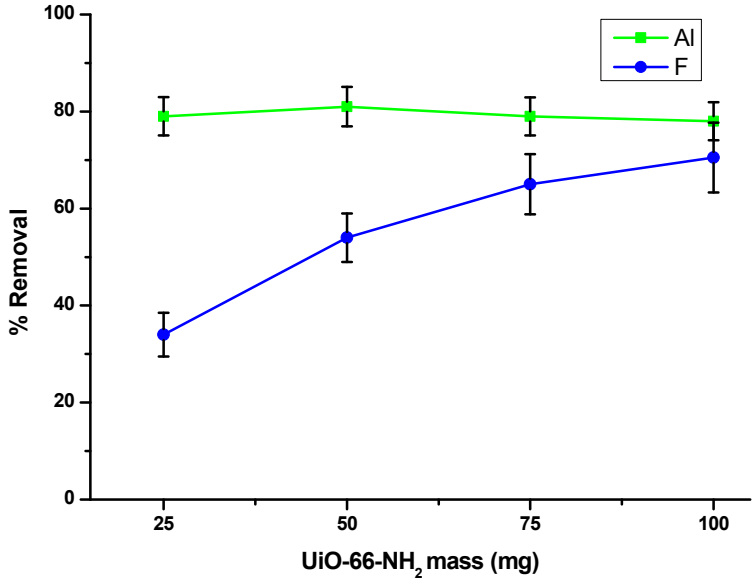

Fig. 5. Comparison of the fluorides and aluminium removal (in %) by different doses of UiO-66-NH_2 in 50 mL of industrial water DW8 (other conditions: [F] = 20 mg/L; [Al] = 0.5 mg/L; contact time = 60 min; n = 2).

The adsorption data of fluorides and aluminium present in DW8 versus contact time are presented in Fig. 6. All the experiments were conducted at industrial pH with the same amount of MOF and the same conditions of the batch. Similar trends were obtained for the two pollutants. As expected, an increase of the adsorption capacity with increasing the contact time was observed. Kinetics also indicated that the adsorption process was uniform with time and can be considered very fast because of the largest amount of pollutant adsorbed to the MOF within the first 15-20 min of adsorption. The remaining concentration of pollutant becomes asymptotic to the time axis after 40 min of stirring. The amount of pollutant adsorbed showed no significant difference when the contact times were longer than this. Fig. 7 compares the removal of fluoride and aluminium by UiO-66-NH_2 and activated carbon materials. It is interesting to note that MOF was able to remove both pollutants simultaneously while activated carbon removed only aluminium. In addition, the Al removal was higher for MOF. The carbon used by the industry is a material with basic properties used on an ad hoc basis to reduce the organic load and metal cations, which is why it is not effective in removing fluorides.

This difference in adsorption capacity could be explained by several mechanisms of fluoride adsorption by UiO-66-NH_2. The material has different possible interaction sites of interaction for fluorides. Firstly, the amino groups present in the linker favour the formation of hydrogen

bonds with fluorides. Secondly, the positive charges on the zirconium cluster, due to the unsaturated coordination, lead to electrostatic interactions with negatively charged ions. Thirdly, the hydroxyl groups present in the Zr cluster also participate in the capture of fluorides. This combination of positive effects may explain the better adsorption of fluoride by UiO-66-NH_2 compared to carbonate materials commonly used in industry [35, 63-65].

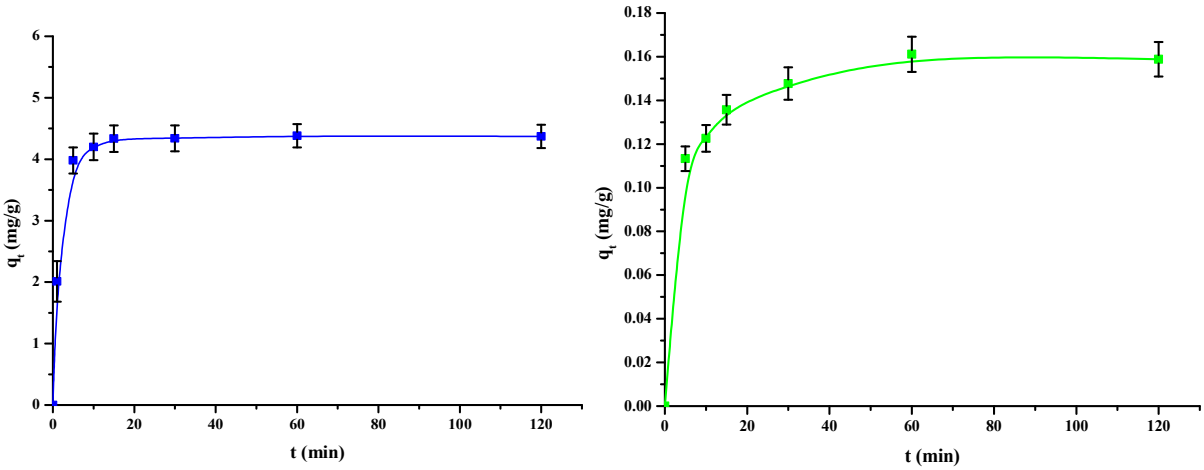

Fig. 6. Comparison of the kinetics of adsorption capacity (expressed in q_t in mg/g) of fluorides (left) and aluminium (right) by UiO-66-NH_2 (other conditions: 100 mg of MOF in 50 mL of industrial water DW8; [F] = 20 mg/L; [Al] = 0.5 mg/L; n = 2).

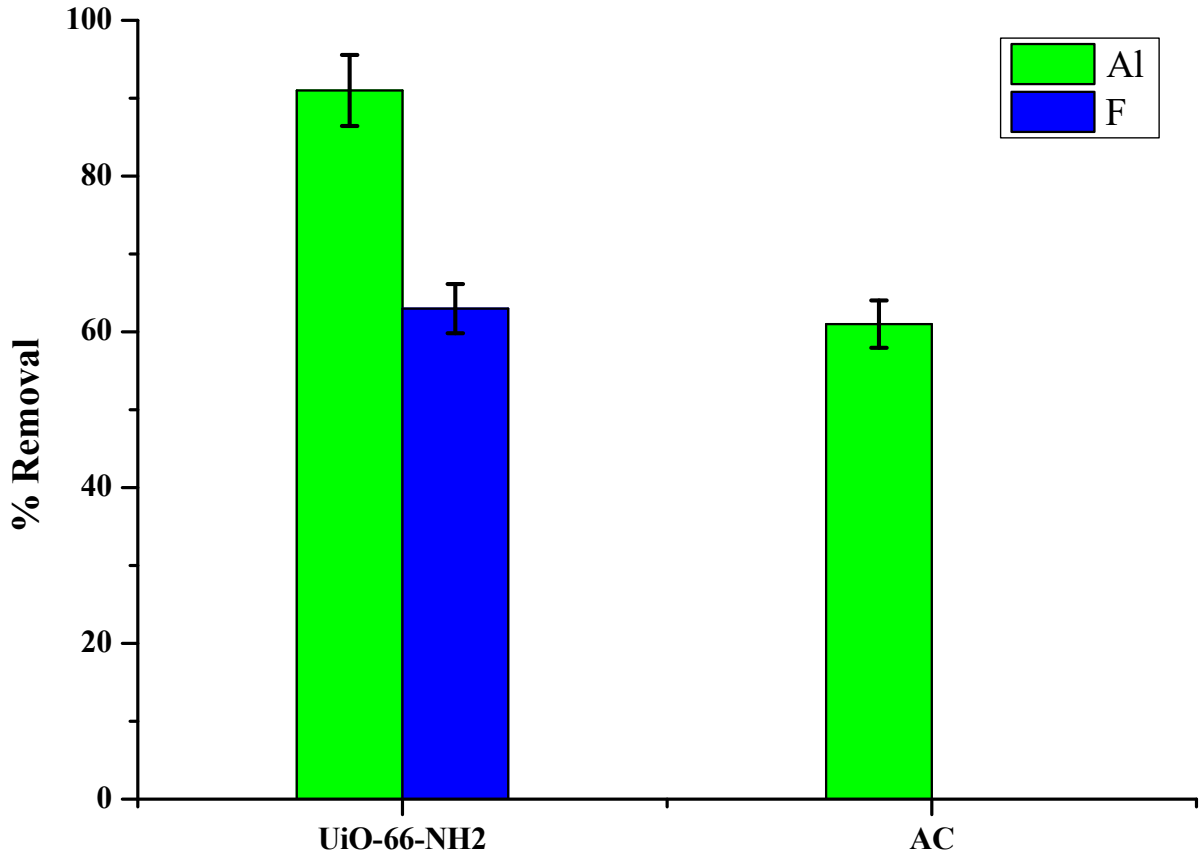

Fig. 7. Comparison of the fluorides and aluminium removal (in %) by UiO-66-NH_2 and activated carbon (AC) in 50 mL of industrial water DW7 (other conditions: 100 mg of material (MOF or AC); [F] = 17 mg/L; [Al] = 0.6 mg/L; contact time = 60 min; n = 3).

3.5 Characterization of materials after adsorption

The XRD and BET analysis and IR spectra were carried out to control the structural and textural properties of UiO-66-NH_2 after adsorption of fluorides and aluminium ions from industrial effluents in dynamic conditions described above. According the XRD diffraction pattern (Fig. 8), the recovered material, having characteristic peaks expressed of UiO-66 family framework with a face-centered-cubic fm3m structure, preserves a high degree of crystallinity. Nevertheless, in parallel of two peaks at 7.4° and 8.5° representing the crystal plane (111) and (002) of UiO crystal structure, two sharp peaks were appeared at 12° and 24° showing the presence of crystalline unidentified impurities adsorbed on zirconium MOF from industrial effluents. The decrease of S_{BET} surface about 30%, from 945 g/m² to 672 g/m² (Fig. 8) confirms also that the impurities are adsorbed by the pores of the UiO-66-NH_2. In other hand, EDX data (Fig. 9) displays the presence of adsorbed metallic ions as aluminium and calcium with a slight change of morphology on SEM images. Compared to the reference (Fig. 2), the particles of UiO-66-NH_2 seems to be less agglomerated, possessing more homogenous size (at x2500).

Fig. 10 gives quantitative results from EDX data before and after adsorption of fluorides and aluminum ions from industrial effluent. However, these percentages obtained are only semi-quantitative. In addition, the error is quite important on this type of analysis (notably because of the roughness of the powders).

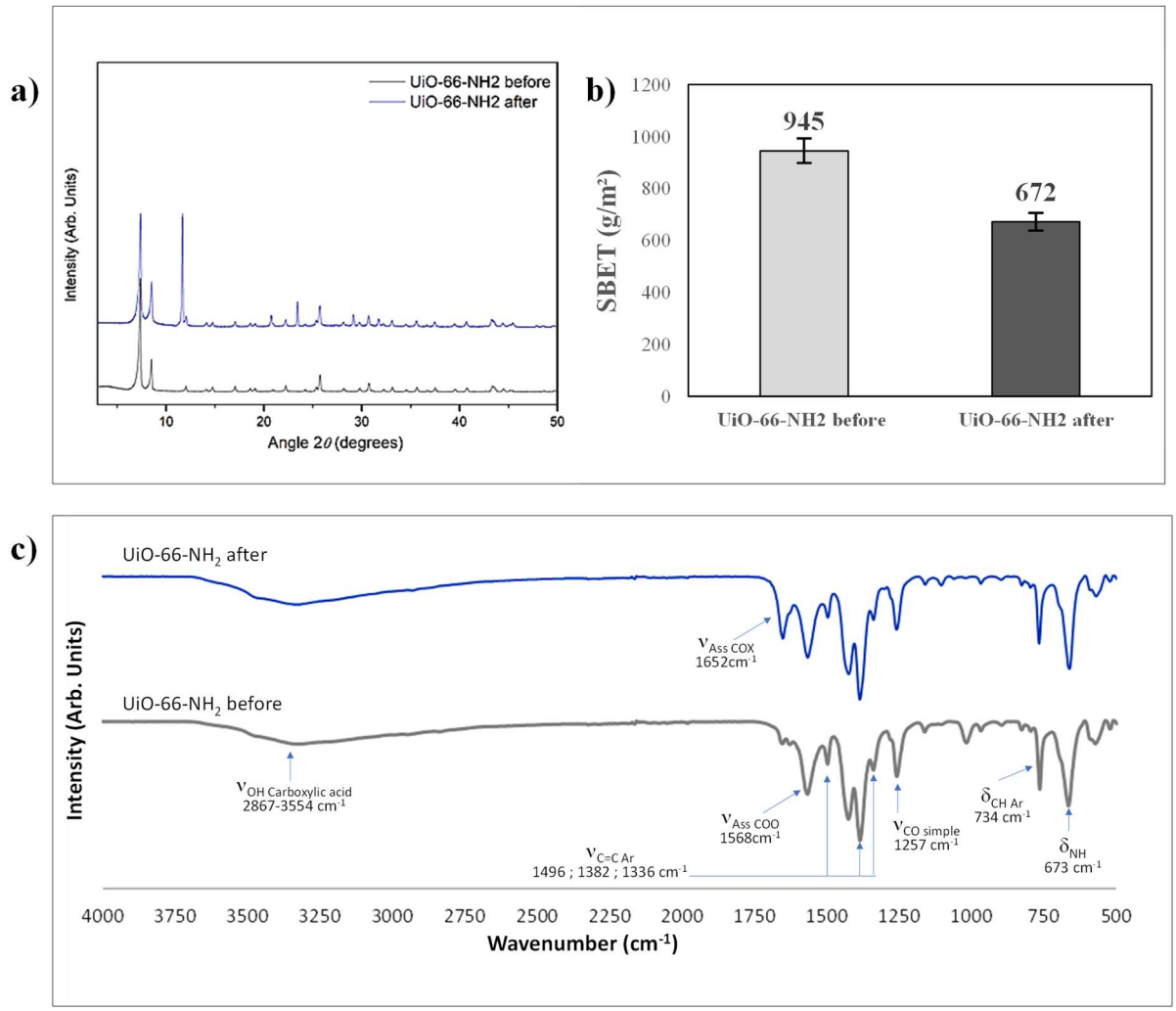

Fig. 8. XRD pattern (a) S_{BET} results (b) and FTIR spectra (c) of UiO-66-NH_2 before and after adsorption of fluorides and aluminium ions from industrial effluent.

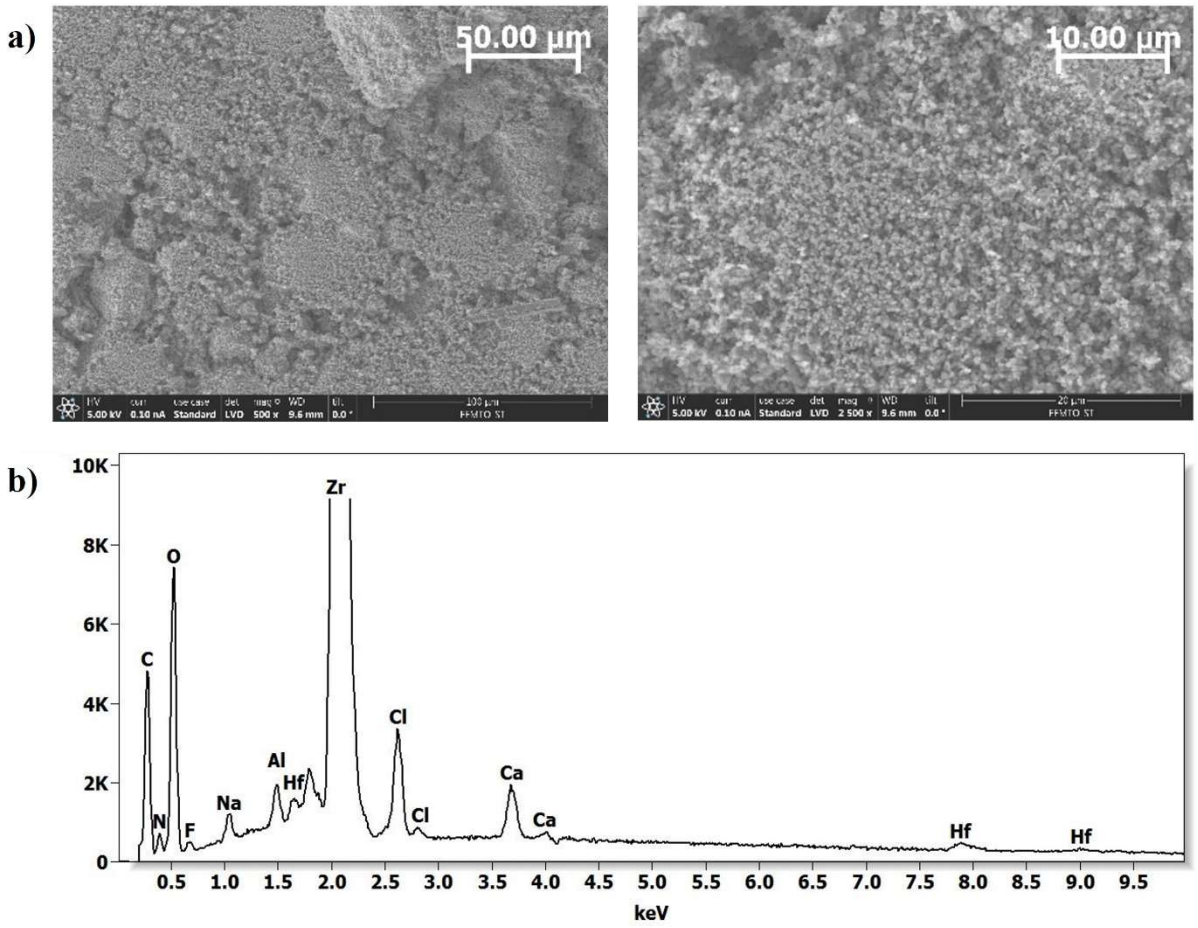

Fig. 9. SEM images at two different magnifications (x500 and x2500) (left) and corresponding EDX data (right) of UiO-66-NH_2 after adsorption of fluorides and aluminium ions from industrial effluent.

a)

Element	Weight %	Atom %
Al	1.69	3.98
Cl	26.35	47.11
Zr	68.74	47.76
Hf	3.21	1.14
Total	100.00	100.00

b)

Element	Weight %	Atom %
F	4.22	13.59
Na	2.19	5.82
Al	2.16	4.89
Cl	11.16	19.27
Ca	4.06	6.19
Zr	73.44	49.28
Hf	2.77	0.95
Total	100.00	100.00

Fig. 10. Quantitative results from EDX data a) before and b) after adsorption of fluorides and aluminium ions from industrial effluent.

The stability of Zr-MOF in water and controlled conditions as a function of pH variation is well documented in the literature [54-62]. However, a lake of data about their behavior in the real industrial effluents have encouraged us to control the stability of our MOF (static conditions described above). The BET and XRD analysis were performed in order to control a textural properties and crystalline structure preservation (Fig. 11). In order to evaluate the possibility of the desorption of the pollutant from the UiO-66-NH_2 after adsorption experiment (2h, 1 day, 1 week), a complementary study was carried out by washing the obtained MOF with water (50 mL x 2) and drying under vacuum at 100 °C for 24 h (Fig. 10). As shown in the XRD patterns, the presence and intensity of characteristics peaks were identical, demonstrating that crystalline structure was preserved after both adsorption experiments (without and with aqueous washing). Besides, no significant changes were observed for specific surface area S_{BET} after adsorption experiment in both conditions (Fig. 10). With the aim of showing the effectiveness and stability of UiO-66-NH_2 in the industrial effluent treatment, the same characterization studies were performed in dynamic conditions (by stirring, described below) to control the evolution of their structural and textural properties.

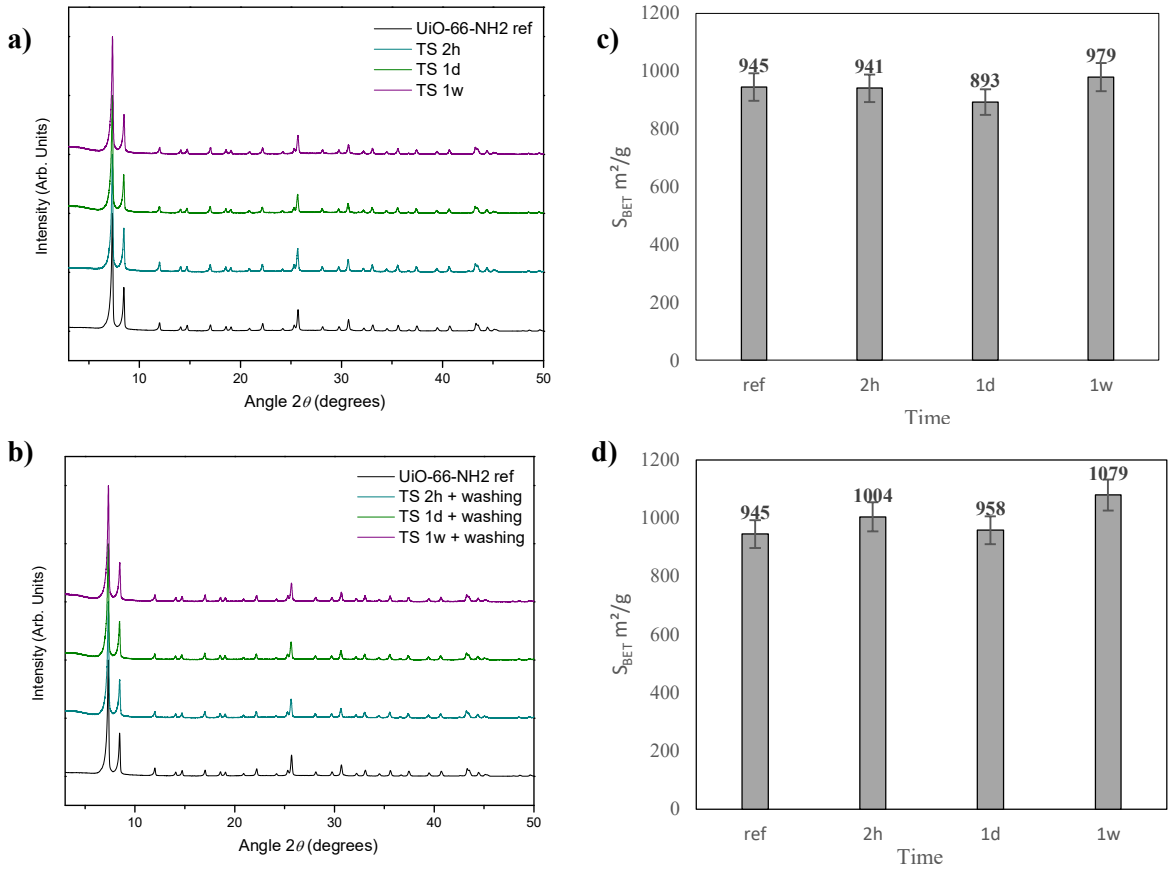

Fig. 11. XRD pattern data (a and b) and S_{BET} results (c and d) of UiO-66-NH_2 before and after industrial effluent adsorption, b and d being obtained after washing (ref = sample before adsorption, 2 h = after 2 h, 1 d = after 1 day, 1w = after 1 week).

4 Conclusion

This contribution reported a study of the use of a highly porous MOF material as adsorbent for the removal of fluorides present in discharge waters from a surface treatment plant. Experimental data indicated that UiO-66-NH_2 was able to remove 70-80% of the fluoride while aluminium was totally eliminated. In both cases, the final concentrations obtained are well below those of the regulatory values, demonstrating the interest of using the process as a complementary treatment to the industrial treatment to further reduce the flow of pollutants. In addition, kinetics are very fast, which is another important aspect for the industrial sector. The next objective of this work will be to prepare large quantities of UiO-66-NH_2 for pilot testing on much larger volumes of water. We have also another ongoing work focused on modeling

results using standardized solutions to compare our results with those published in the literature (Table 3).

Table 3

Reported maximum adsorption capacity (q_{max} in mg/g) of UiO-66 and UiO-66-NH_2 MOFs for fluorides.

MOFs	pH	q_{max}	Mechanism	Reference
UiO-66	6.8	41.36	electrostatic interactions	[40]
UiO-66		41.2	electrostatic interactions	[35]
UiO-66-NH_2		52.6	electrostatic interactions	[35]
UiO-66-NH_2	6.1	49.7	electrostatic interactions	This work
UiO-66-NH_2	7	41.5	electrostatic interactions	[46]
UiO-66-NH_2	6.5	26.53	electrostatic interactions	[62]

Credit authorship contribution statement

GC, AP and JR supervised the project. DL, GH, CM, and NMC realized the experiments. CR, CL, MR, EM, and VP performed the material characterization. The manuscript was written through contributions of all authors. All authors have given approval to the final version of the manuscript.

Declaration of competing interest

The authors declare no competing financial interest.

Acknowledgements

The authors thank *Silac Industrie* (Champlitte, France), *Région Bourgogne Franche-Comté*, and *Université de Franche-Comté* (FLUOREX and CHRYSALIDE Projects) for financial support, and the PEA^2t Plateform (Chrono-environnement, Besançon, U*niversité de Franche-Comté*, MYDREAU Project) which manages and maintains the analytical equipment used in this work. Dario Lacalamita and Chiara Mongioví thanks the *Région Bourgogne Franche-Comté* for awarding them a research grant (FINEAU Project). The authors also acknowledge the scientific and technical expertise of Xavier Hutinet and Elise Euvrard (*Silac Industrie*, Champlitte, France). Finally, the authors would also like to thank the Editor and the four anonymous reviewers: we appreciated all their constructive comments and suggestions for improving the paper.

References

[1] G.A. Udourioh, M.M. Solomon, C.O. Matthews-Amune, E.I. Epelle, J.A. Okolie, V.E. Agbazue, U. Onyenze. Current trends in the synthesis, characterization and application of metal-organic frameworks. Reaction Chem. Eng. 8 (2023) 278-310, https://doi.org/10.1039/D2RE00365A.

[2] F. Bi, Z. Zhao, Y. Yang, W. Gao, N. Liu, Y. Huang, X. Zhang. Chlorine-coordinated Pd single atom enhanced the chlorine resistance for volatile organic compound degradation: Mechanism study. Environ. Sci. Technol. 56 (2022) 17321-17330, https://doi.org/10.1021/acs.est.2c06886.

[3] Q. Zhao, Z. Zhao, R. Rao, Y. Yang, S. Ling, F. Bi, X. Shi, J. Xu, G. Lu, X. Zhang. Universitetet i Oslo-67 (UiO-67)/graphite oxide composites with high capacities of toluene: Synthesis strategy and adsorption mechanism insight. J. Colloid Int. Sci. 627 (2022) 385-397, https://doi.org/10.1016/j.jcis.2022.07.059.

[4] Hitabatuma A, Wang PL, Su XO, Ma MM. Metal-organic frameworks-based sensors for food safety. Foods 11 (2022) 382, https://doi.org/10.3390/foods11030382.

[5] G. Rando, S. Sfameni, M. Galetta, D. Drommi, S. Cappello, M.R. Plutino. Functional nanohybrids and nanocomposites development for the removal of environmental pollutants and bioremediation. Molecules 27 (2022) 4856, https://doi.org/10.3390/molecules27154856.

[6] A. Al Obeidli, H.B. Salah, M. Al Murisi, R. Sabouni. Recent advancements in MOFs synthesis and their green applications. Int. J. Hydrogen Energy 47 (2022) 2561-2593, https://doi.org/10.1016/j.ijhydene.2021.10.180.

[7] Q.S. Miao, L.R. Jiang, J. Yang, T.D. Hu, S.Y. Shan, Su H.G., F. Wu. MOF/hydrogel composite-based adsorbents for water treatment: A review. J. Water Process Eng. 50 (2022) 103348, https://doi.org/10.1016/j.jwpe.2022.103348.

[8] Bag PP, Singh GP, Singha S, Roymahapatra G. Synthesis of metal-organic frameworks (MOFs) and their biological, catalytic and energetic application: A mini review. Engineered Sci. 13 (2021) 1-10, https://doi.org/10.30919/es8d1166.

[9] T. Rasheed, A.A. Hassan, M. Bilal, T. Hussain, K. Rizwan. Metal-organic frameworks based adsorbents: A review from removal perspective of various environmental contaminants from wastewater. Chemosphere 259 (2020) 127369, https://doi.org/10.1016/j.chemosphere.2020.127369.

[10] Kumar S, Jain S, Nehra M, Dilbaghi N, Marrazza G, Kim KH. Green synthesis of metal-organic frameworks: A state-of-the-art review of potential environmental and medical applications. Coordination Chem. Rev. 420 (2020) 213407, https://doi.org/10.1016/j.ccr.2020.213407.

[11] Wang B., Xie L.H., Wang X., Liu X.M., Li J., Li J.R. Applications of metal-organic frameworks for green energy and environment: New advances in adsorptive gas separation, storage and removal. Green Energy Environ. 3 (2018) 191-228, https://doi.org/10.1016/j.gee.2018.03.001.

[12] A. Al Obeidli, H.B. Salah, M. Al Murisi, R. Sabouni. Recent advancements in MOFs synthesis and their green applications. Int J Hydrogen Energy 47 (2022) 2561-2593, https://doi.org/10.1016/j.ijhydene.2021.10.180.

[13] Safaei M, Foroughi MM, Ebrahimpoor N, Jahani S, Omidi A, Khatami M. A review on metal-organic frameworks: Synthesis and applications. Trends Anal. Chem. 118 (2019) 401-425, https://doi.org/10.1016/j.trac.2019.06.007.

[14] S. Yuan, L. Feng, K. Wang, J. Pang, M. Bosch, C. Lollar, Y. Sun, J. Qin, X. Yang, P. Zhang, Q. Wang, L. Zou, Y. Zhang, L. Zhang, Y. Fang, J. Li, H.C. Zhou. Stable metal-organic frameworks: design, synthesis, and applications. Adv. Mater. 30 (2018) 1704303, https://doi.org/10.1002/adma.201704303.

[15] P. Kumar, V. Bansal, K.H. Kim, E.E. Kwon. Metal-organic frameworks (MOFs) as futuristic options for wastewater treatment. J. Ind. Eng. Chem. 62 (2018) 130-145, https://doi.org/10.1016/j.jiec.2017.12.051.

[16] M. Mon, R. Bruno, J. Ferrando-Soria, D. Armentano, E. Pardo. Metal-organic framework technologies for water remediation: towards a sustainable ecosystem. J. Mater. Chem. A 6 (2018) 4912-4947, https://doi.org/10.1039/C8TA00264A.

[17] L. Joseph, B.M. Jun, M. Jang, C.M. Park, J.C. Muñoz-Senmache, A.J. Hernández-Maldonado, A. Heyden, M. Yu, T. Yoon. Removal of contaminants of emerging concern by metal-organic framework nanoadsorbents: A review. Chem. Eng. J. 369 (2019) 928-946, https://doi.org/10.1016/j.cej.2019.03.173.

[18] J. Wen, Y. Fang, G. Zeng. Progress and prospect of adsorptive removal of heavy metal ions from aqueous solution using metal-organic frameworks: A review of studies from the last decade. Chemosphere 201 (2018) 627-643, https://doi.org/10.1016/j.chemosphere.2018.03.047.

[19] S. Rojas, P. Horcajada. Metal-organic frameworks for the removal of emerging organic contaminants in water. Chem. Rev. 120 (2020) 8378-8415, https://doi.org/10.1021/acs.chemrev.9b00797.

[20] Z.U. Zango, K. Jumbri, N.S. Sambudi, A. Ramli, N.H.H. Abu Bakar, B. Saad, M.N.H. Rozaini, H.A. Isiyaka, A.H. Jagaba, O. Aldaghri, A. Sulieman. A critical review on metal-organic frameworks and their composites as advanced materials for adsorption and photocatalytic degradation of emerging organic pollutants from wastewater. Polymers 12 (2020) 2648, https://doi.org/10.3390/polym12112648.

[21] J. Ru, X. Wang, F. Wang, X. Cui, X. Du, X. Lu. UiO series of metal-organic frameworks composites as advanced sorbents for the removal of heavy metal ions: Synthesis, applications and adsorption mechanism. Ecotoxicol. Environ. Safety 208 (2021) 111577, https://doi.org/10.1016/j.ecoenv.2020.111577.

[22] X. G. Liu, Y.Y. Shan, S.T. Zhang, Q.Q. Kong, H. Pang. Application of metal-organic framework in wastewater treatment. Green Energy Environ. (2022) https://doi.org/10.1016/j.gee.2022.03.005.

[23] C.C. Yan, J.Q. Jin, J. Wang, F.F. Zhang, Y.J. Tian, C.X. Liu, F.Q. Zhang, L.C. Cao, Y.M. Zhou, Q.X. Han. Metal-organic frameworks (MOFs) for the efficient removal of contaminants from water: Underlying mechanisms, recent advances, challenges, and future prospects. Coordination Chem. Rev. 468 (2022) 214595, https://doi.org/10.1016/j.ccr.2022.214595.

[24] I. Ihsanullah. Applications of MOFs as adsorbents in water purification: Progress, challenges and outlook. Current Opinion Environ. Sci. Health 26 (2022) 100335, https://doi.org/10.1016/j.coesh.2022.100335.

[25] Daglar H, Altintas C, Erucar I, Heidari G, Zare EN, Moradi O, Srivastava V, Iftekhar S, Keskin S, Sillanpää M. Metal-organic framework-based materials for the abatement of air pollution and decontamination of wastewater. Chemosphere 303 (2022) 135082, https://doi.org/10.1016/j.chemosphere.2022.135082.

[26] N. Abdollahi, G. Moussavi, S. Giannakis. A review of metal's removal from aqueous matrices by metal-organic frameworks (MOFs): State-of-the-art and recent advances. J. Environ. Chem. Eng. 10 (2022) 107394, https://doi.org/10.1016/j.jece.2022.107394.

[27] J. Darabdhara, M. Ahmaruzzaman. Recent developments in MOF and MOF based composite as potential adsorbents for removal of aqueous environmental contaminants. Chemosphere 304 (2022) 135261, https://doi.org/10.1016/j.chemosphere.2022.135261.

[28] B. Abdollahi, D. Salari, M. Zarei. Synthesis and characterization of magnetic Fe_3O_4@SiO_2-MIL-53(Fe) metal-organic framework and its application for efficient removal of arsenate from surface and groundwater. J. Environ. Chem. Eng. 10 (2022) 107144, https://doi.org/10.1016/j.jece.2022.107144.

[29] M.A. Gatou, P. Bika, T. Stergiopoulos, P. Dallas, E.A. Pavlatou. Recent advances in covalent organic frameworks for heavy metal removal applications. Energies 14 (2021) 3197, https://doi.org/10.3390/en14113197.

[30] Z.W. Li, L. Wang, L. Qin, C. Lai, Z.H. Wang, M. Zhou, L.H. Xiao, S.Y. Liu, M.M. Zhang. Recent advances in the application of water-stable metal-organic frameworks: Adsorption and photocatalytic reduction of heavy metal in water. Chemosphere 285 (2021) 131432, https://doi.org/10.1016/j.chemosphere.2021.131432.

[31] A. Wibowo, M.A. Marsudi, E. Pramono, J. Belva, A.W.Y.P. Parmita, A. Patah, D. Eddy, A.H. Aimon, A. Ramelan. Recent improvement strategies on metal-organic frameworks as adsorbent, catalyst, and membrane for wastewater treatment. Molecules 26 (2021) 5261, https://doi.org/10.3390/molecules26175261.

[32] X. Zhao, X. Yu, X. Wang, S. Lai, Y. Sun, D. Yang. Recent advances in metal-organic frameworks for the removal of heavy metal oxoanions from water. Chem. Eng. J. 407 (2021) 127221, https://doi.org/10.1016/j.cej.2020.127221.

[33] K.A. Adegoke, O.S. Agboola, J. Ogunmodede, A.O. Araoye, O.S. Bello. Metal-organic frameworks as adsorbents for sequestering organic pollutants from wastewater. Mater. Chem. Phys. 253 (2020) 123246, https://doi.org/10.1016/j.matchemphys.2020.123246.

[34] M. Feng, P. Zhang. H.C. Zhou, V.K. Sharma. Water-stable metal-organic frameworks for aqueous removal of heavy metals and radionuclides: A review. Chemosphere 209 (2018) 783-800, https://doi.org/10.1016/j.chemosphere.2018.06.114.

[35] K.Y.A. Lin, Y.T. Liu, S.Y. Chen. Adsorption of fluoride to UiO-66-NH_2 in water: stability, kinetic, isotherm and thermodynamic studies. J. Colloid Int. Sci. 461 (2016) 79-87, https://doi.org/10.1016/j.jcis.2015.08.061.

[36] S. Dhaka, R. Kumar, A. Deep, M.B. Kurade, S.W. Ji, B.H. Jeon. Metal-organic frameworks (MOFs) for the removal of emerging contaminants from aquatic environments. Coordination Chem. Rev. 380 (2019) 330-352, https://doi.org/10.1016/j.ccr.2018.10.003.

[37] D. Jiang, M. Chen, H. Wang, G. Zeng, D. Huang, M. Cheng, Y. Liu, W. Xue, Z.W. Wang. The application of different typological and structural MOFs-based materials for the dyes adsorption. Coordination Chem. Rev. 380 (2019) 471-483, https://doi.org/10.1016/j.ccr.2018.11.002.

[38] K.A. Adegoke, O.S. Agboola, J. Ogunmodede, A.O. Araoye, O.S. Bello. Metal-organic frameworks as adsorbents for sequestering organic pollutants from wastewater. Mater. Chem. Physics 253 (2020) 123246, https://doi.org/10.1016/j.matchemphys.2020.123246.

[39] V.K.M. Au. Recent advances in the use of metal-organic frameworks for dye adsorption. Frontiers Chem. 8 (2020) 708, https://doi.org/10.3389/fchem.2020.00708.

[40] F. Ahmadijokani, H. Molavi, M. Rezakazemi, S. Tajahmadi, A. Bahi, K. Ko, T.M. Aminabhavi, J.R. Li, M. Arjmand. UiO-66 metal-organic frameworks in water treatment: A critical review. Prog. Mater. Sci. 125 (2022) 100904, https://doi.org/10.1016/j.pmatsci.2021.100904.

[41] F. Ahmadijokani, H. Molavi, M. Rezakazemi, T.M. Aminabhavi, M. Arjmand. Simultaneous detection and removal of fluoride from water using smart metal-organic framework-based adsorbents. Coordination Chem. Rev. 445 (2021) 214037, https://doi.org/10.1016/j.ccr.2021.214037.

[42] L. Huang, R. Shen, Q. Shuai. Adsorptive removal of pharmaceuticals from water using metal-organic frameworks: A review. J. Environ. Manag. 277 (2021) 111389, https://doi.org/10.1016/j.jenvman.2020.111389.

[43] X. Zhang, M. Liu, R. Han. Adsorption of phosphate on UiO-66-NH_2 prepared by a green synthesis method. J. Environ. Chem. Eng. 9 (2021) 106672, https://doi.org/10.1016/j.jece.2021.106672.

[44] X. Zhao, Z. Zheng, X. Gao, J. Zhang, E. Wang, Z. Gao. The application of MOFs-based materials for antibacterials adsorption. Coordination Chem. Rev. 440 (2021) 213970, https://doi.org/10.1016/j.ccr.2021.213970.

[45] G. Sriram, A. Bendre, E. Mariappan, T. Altalhi, M. Kigga, Y.C. Ching, H.Y. Jung, B. Bhaduri, M. Kurkuri. Recent trends in the application of metal-organic frameworks (MOFs) for the removal of toxic dyes and their removal mechanism-a review. Sustainable Mater. Technol. 31 (2022) e00378, https://doi.org/10.1016/j.susmat.2021.e00378.

[46] M. Massoudinejad, M. Ghaderpoori, A. Shahsavani, M.M. Amini. Adsorption of fluoride over a metal organic framework UiO-66 functionalized with amine groups and optimization with response surface methodology. J. Molecular Liq. 221 (2016) 279-286, https://doi.org/10.1016/j.molliq.2016.05.087.

[47] A. Mohamed, E.P.V. Sanchez, E. Bogdanova, B. Bergfeldt, A. Mahmood, R.V. Ostvald T. Hashem. Efficient fluoride removal from aqueous solution using zirconium-based composite nanofiber membranes. Membranes 11 (2021) 147, https://doi.org/10.3390/membranes11020147.

[48] L.P. Wang, X.R. Dai, Z. Man, J.R. Li, Y.F. Jiang, D.Z. Liu, H. Xiao, S. Shah. Dynamics and treatability of heavy metals in pig farm effluent wastewater by using UiO-66 and UiO-66-NH_2 nanomaterials as adsorbents. Water Air Soil Pollut. 232 (2021) 294, https://doi.org/10.1007/s11270-021-05229-6.

[49] G. Crini, E. Lichtfouse. Advantages and disadvantages of techniques used for wastewater treatment. Environ. Chem. Lett. 17 (2019) 145-155, https://doi.org/10.1007/s10311-018-0785-9.

[50] G. Hoyez, J. Rousseau, C. Rousseau, S. Saitzek, J. King, P. Ágota Szilágyi, C. Volkringer, T. Loiseau, F. Hapiot, E. Monflier, A. Ponchel. Cyclodextrins: a new and effective class of co-modulators for aqueous zirconium-MOF syntheses. CrystEngComm 23 (2021) 2764-2772, https://doi.org/10.1039/D1CE00128K.

[51] F. Rouquerol, J. Rouquerol, K. Sing. Adsorption by powders & porous solids. Principles, methodology and applications, Academic Press, London, 1999, pp79-83.

[52] J. Charles, G. Crini, C. Bradu, G. Torri, S. Gavoille, B. Sancey, N. Morin-Crini, G. Trunfio, P.M. Badot, P. Winterton, C. Lagarrigue. Optimisation of an industrial wastewater decontamination plant: An environment-oriented approach. Canadian J. Chem. Eng. 92 (2014) 391-400, https://doi.org/10.1002/cjce.21857.

[53] B. Sancey, J. Charles, G. Trunfio, P.M. Badot, M. Jacquot, X. Hutinet, S. Gavoille, G. Crini. Effect of additional sorption treatment by cross-linked starch of wastewater from a surface finishing plant. Ind. Eng. Chem. Res. 50 (2011) 1749-1756, https://doi.org/10.1021/ie1010492.

[54] H. Reinsch, S. Waitschat, S.M. Chavan, K.P. Lillerud, N. Stock. A facile 'green' route for scalable batch production and continuous synthesis of zirconium MOFs. European J. Inorganic Chem. 27 (2016) 4490-4498, https://doi.org/10.1002/ejic.201600295.

[55] E. Moumen, A.H. Assen, K. Adil, Y. Belmabkhout. Versatility vs stability. Are the assets of metal-organic frameworks deployable in aqueous acidic and basic media? Coordination Chem. Rev. 443 (2021) 214020, https://doi.org/10.1016/j.ccr.2021.214020.

[56] D. Bůžek, S. Adamec, K. Lang, J. Demel. Metal-organic frameworks vs. buffers: case study of UiO-66 stability. Inorganic Chem. Frontiers 8 (2021) 720-734, https://doi.org/10.1039/D0QI00973C.

[57] K. Leus, T. Bogaerts, J. De Decker, H. Depauw, K. Hendrickx, H. Vrielinck, V. Van Speybroeck, P. Van Der Voort. Systematic study of the chemical and hydrothermal stability of selected "stable" metal organic frameworks. Microporous Mesoporous Mater. 226 (2016) 110-116, https://doi.org/10.1016/j.micromeso.2015.11.055.

[58] C.G. Piscopo, A. Polyzoidis, M. Schwarzer, S. Loebbecke. Stability of UiO-66 under acidic treatment: Opportunities and limitations for post-synthetic modifications. Microporous Mesoporous Mater. 208 (2015) 30-35, https://doi.org/10.1016/j.micromeso.2015.01.032.

[59] N. Ul Qadir, S.A.M. Said, H.M. Bahaidarah. Structural stability of metal organic frameworks in aqueous media - Controlling factors and methods to improve hydrostability and hydrothermal cyclic stability. Microporous Mesoporous Mater. 201 (2015) 61-90, https://doi.org/10.1016/j.micromeso.2014.09.034.

[60] H.Y. Wang, L.J. Hou, Y.J. Shen, L. Huang, Y.J. He, W.C. Yang, T. Yuan, J. Linfeng, C.J. Tang, L.Y. Zhang. Synthesis of core-shell UiO-66-poly(m-phenylenediamine) composites for removal of hexavalent chromium. Environ. Sci. Pollut. Res. 27 (2020) 4115-4126, https://doi.org/10.1007/s11356-019-07070-1.

[61] Y.R. Wang, J.L. Yin, W.C. Cao, Y. Fu, X.Q. Kong. The instability of a stable metal-organic framework in amino acid solutions. Nano Res. 15 (2022) 6607-6612, https://doi.org/10.1007/s12274-022-4346-y.

[62] S.B. Wu, J. Yang, Y. Xu, X. Chen, Y.J. Ge, W.S. Zou, S.H. Chen, H.Y. Xu. Enhanced adsorption of fluoride on nano UiO-66-NH_2 MOF in water. Fresenius Environ. Bull. 28 (2019) 5466-5473.

[63] X. Tang, C. Zhou, W. Xia, Y. Liang, Y. Zeng, X. Zhao, W. Xiong, M. Cheng, Z. Wang. Recent advances in metal-organic framework-based materials for removal of fluoride in water: Performance, mechanism, and potential practical application. Chem. Eng. J. 446 (2022) 137299. https://doi.org/10.1016/j.cej.2022.137299.

[64] H. Fei, J. Shin, Y.S. Meng, M. Adelhardt, J. Sutter, K. Meyer, S.M. Cohen. Reusable oxidation catalysis using metal-monocatecholato species in a robust metal-organic framework. J. Am. Chem. Soc. 136 (2014) 4965-4973, https://doi.org/10.1021/ja411627z.

[65] J. Hou, H. Wang, H. Zhang. Zirconium metal-organic framework materials for efficient ion adsorption and sieving. Ind. Eng. Chem. Res. 59 (2020) 12907-12923, https://doi.org/10.1021/acs.iecr.0c02683.